UDC 54.544.6

# THE LATEST PROGRESS ON SYNTHESIS AND INVESTIGATION OF $Sb_2S_3$-BASED THIN FILMS

**V.A. Majidzade, S.F. Jafarova, S.P. Javadova, A.Sh. Aliyev, D.B. Tagiyev**

*Acad. M. Nagiyev Institute of Catalysis and Inorganic Chemistry*
*Ministry of Science and Education of the Republic of Azerbaijan*
*AZ 1143, H. Javid Ave. 113, Baku, Azerbaijan*
*e-mail: vuska_80@mail.ru*

*Received 15.02.2023*
*Accepted 12.06.2023*

***Abstract:*** *$Sb_2S_3$ is stable under environmental conditions and a promising semiconductor material for optoelectronic applications, its potential capabilities in solar cells, photodetectors, and other devices are being investigated. It has an indirect-band gap of approximately 1.7-1.9 eV depending on the crystal structure which makes it suitable for absorption of visible light and its use in solar batteries. $Sb_2S_3$ can exist in different crystal structures including orthorhombic and hexagonal structures. The crystal structure can significantly affect the electronic and optical properties, which makes it possible to adapt its properties for specific applications using crystal structure engineering. It also has great optical properties and high absorption coefficients in the visible and near-infrared regions of the spectrum and makes it suitable for use in photogalvanics and photodetectors. Although there are various methods for obtaining this material, further research and development are needed to optimize its properties, improve productivity, and explore new applications.*

***Keywords:*** *semiconductors, $Sb_2S_3$, electrodeposition, thin films, properties of $Sb_2S_3$ films*
***DOI: 10.32737/2221-8688-2023-2-99-122***

## Introduction

Functional thin films are thin layers of materials that have specific physical, chemical or electronic properties. They are widely used in various fields of science and technology, including electronics, optics, photonics, catalysis, sensorics, medicine, etc. It is important to emphasize that the properties of such thin metal chalcogenide films can be carefully adjusted and optimized by controlling their thickness, composition and microstructure. This makes it possible to obtain materials with unique properties that can be used to develop new devices and technologies [1-17].

In terms of designing and manufacturing devices, thin-film technology has made solar cells more convenient to use. But the efficiency of these solar cells still needs to be improved. A lot of studies were carried out in line with this objective. So, developments in the searching range of innovative materials proceed on their way in thin-film solar cells for the development of the photoelectric field due to increasing its efficiency [18]. One such innovative material is antimony-based thin films.

Antimony films have a silver-white color and are represented as brittle metal coatings [19]. Pure, unalloyed antimony is rarely used in industry, but its alloys and chemical compounds are widely used. Antimony is a constituent component of alloys such as $Cu_2Sb$, SnSb, AlSb, $CoSb_3$, $ZnSb_3$, InSb and $InAs_{1-x}Sb_x$. In addition, antimony is a component of many semiconductor compounds used in solar cells and humidity sensors that due to their thermoelectric properties, are used in the manufacture of thermoelectric generators, thermal batteries, and microcoolers [20-29].

$Sb_2S_3$ thin films can have both p- and n-type conductivity depending on their obtaining method [30, 31].

$Sb_2S_3$ thin films are widely used in various devices, including solar cells [32-39]. Antimony sulfide $Sb_2S_3$ is an important semiconductor [40]. This compound was studied quite widely for its potential usage in optoelectronic devices, microwave devices and photovoltaic structures [41-43]. It occurs in nature as a stibnite mineral with a rhombic crystal structure. Its special properties such as high refractive index, distinct quantum-size effect, photosensitivity and thermoelectric properties make this material suitable for the above-mentioned fields.

The use of $Sb_2S_3$ and $Sb_2Se_3$ in the solar cell structure is related to their optical properties [26, 44-46]. The optical band gap for $Sb_2S_3$ crystalline thin films is in the range of 1.6 to 1.8 eV. The films have a high absorption coefficient [44-46]. For example, $Sb_2S_3$ thin film with a thickness of 1 μm can absorb nearly 95% of solar radiation [47]. Besides, the components of this compound are abundant in nature, which attracts the attention of researchers to this material as a photoelectric absorber. Over the last few years, intensive efforts were made to improve the photovoltaic efficiency of $Sb_2S_3$-based solar cells using many promising approaches, including interfacial engineering, surface passivation, additive engineering, and band gap engineering of charge transfer layers and $Sb_2S_3$ materials absorbing the active light [48]. Both structural and morphological changes in $Sb_2S_3$ thin films affecting the current state of development of $Sb_2S_3$-based solar cells were studied to understand and improve the device operation [49].

## Thermal Deposition Methods

One of the earliest methods for producing $Sb_2S_3$ thin films is the thermal method. In [50], the report presents studies carried out in order to obtain crystalline thin films of $Sb_2S_3$ by spray pyrolysis. Aqueous and mixed solvents (water-ethanol) were selected for the studies using antimony (III) ($CH_3COO$) acetate (3Sb) and thiourea $H_2NCSNH_2$ as precursors in a weight ratio of 1:2. A small amount of HCl is used to increase the solubility of the $(CH_3COO)_3Sb$ and prevent precipitation of $Sb_2S_3$ in aqueous solution by forming $Sb(OH)_3$ in the form of white precipitate. Deposits were obtained by changing deposition parameters: deposition temperature, number of sequences and solvent type (water or mixed solvent: water-ethanol). The obtained data were analyzed by methods of X-ray diffraction, atomic force microscopy, UV-spectroscopy and volt-ampere measurements under dark and visible-light conditions. The analysis results are indicative of the formation of $Sb_2S_3$ crystalline thin films with electrical properties that can be used as a buffer layer or as an absorbent material in three-dimensional cells. The effect of heat treatment for 30 minutes due to temperature range from 300 K to 473 K on the structural, electrical and optical properties of thin films of antimony trisulfide ($Sb_2S_3$) was studied [51]. Thin films deposited on a glass substrate heated up to 300 K by vacuum thermal evaporation had an amorphous structure. After annealing, the structure of the films changed to polycrystalline, while the films deposited on the substrate at 498 K temperature had a polycrystalline structure both before and after heat treatment [51].

In [52], $Sb_2S_3$ thin films were also obtained by thermal evaporation. The deposited films were amorphous, while the plasma-treated and annealed at 250°C for 2 hours had a rhombic microcrystalline structure.

At room temperature, $Sb_2S_3$ thin films of different thicknesses were applied to pure glass substrates coated with indium and tin oxide (ITO) by thermal evaporation [53]. The films had an amorphous structure that turned into a polycrystalline structure after heat treatment.

$Sb_2S_3$ and $(Sb_2S_3)_{0,9}Se_{0,1}$ thin films were obtained on the microscope glass slides at room temperature by thermal vacuum evaporation and electron beam deposition. The effect of selenium doping on the structural, optical and electrical properties of $Sb_2S_3$ thin films was investigated [54].

$Sb_2S_3$ thin films were covered to glass substrates by vacuum thermal evaporation [55-57] wherein a substrate temperature ranged from 30°C to 240°C. Ground powder of synthesized $Sb_2S_3$ was used as raw material for vacuum thermal evaporation.

The structural study showed that the films have an amorphous structure, and the analysis of the absorption coefficient revealed two direct forbidden zones 1.78 - 1.98 eV and 1.86 - 2.08 eV [55]. X-ray diffraction (XRD) showed that the films deposited on the TS substrate < 250°C had an amorphous structure and the films obtained at TS ≥250°C were polycrystalline [56]. In the [58] report, $Sb_2S_3$ films were applied by thermal evaporation using the glancing angle deposition technique. Stoichiometric amounts of elements antimony Sb and sulfur S with a purity of 99.999% were used as starting materials. The temperature of the substrate was maintained at 180°C and the deposition angle varied from 0° to 85°.

The authors noted [59] that the glass substrates were purified with a solution of hydrofluoric acid containing various ratios (from 0 to 100%) of ammonium fluoride and water, then they were subjected to chemical etching, and only after that, $Sb_2S_3$ thin films were applied to them by vacuum thermal evaporation at the substrate temperature of 300K. The films obtained like that had the best photovoltaic properties.

It was found that the surface roughness of etched glass substrates varies depending on the concentration of $F^-$ ions in the solution and the etching time. Since it is that good crystallization and orientation of films affect the conversion efficiency of solar cells, so this procedure of highly oriented-thin film growth of $Sb_2S_3$ is very important. $Sb_2S_3$ thin films were obtained at 250°C on glass substrates by spray pyrolysis [60]. Structural and X-ray phase analysis of the resulting films was conducted. Article [61] describes the synthesis of thin films of antimony sulfide ($Sb_2S_3$) by thermal evaporation and the detailed characteristics of these films. The film was applied from $Sb_2S_3$ powder to the surface of the substrate. The structural, optical, morphological and electrical properties of sputtered $Sb_2S_3$ films annealed and unannealed in a nitrogen atmosphere in the temperature range of 100-300°C were examined. Films of both amorphous and polycrystalline antimony sulfide have strong absorption coefficients in the range of $10^4 \div 5\times10^5$ cm$^{-1}$ and have directly forbidden zones with energy bands of 2.0-2.2 eV for films annealed below 200°C, and 1.7-1.8 eV for films annealed above 200°C.

$Sb_2S_3$ thin films obtained by flash evaporation were amorphous, but after annealing in a nitrogen atmosphere at a temperature of 498K, they turned into the polycrystalline form [62]. The optical transition is straight; the optical band gap ($E_q$) for amorphous and crystalline films between in the region of 1.7-2.7 eV and 1.42-1.65 eV, respectively. The band gap depends on the S/Sb ratio of the film composition.

$Sb_2S_3$ thin films were obtained from thiourea (CS $(NH_2)_2$) and antimony trichloride ($SbCl_3$) by spray pyrolysis [63]. The morphology of the film surface was analyzed using atomic force microscopy (AFM). Analysis of the optical constants of the obtained films made it possible to determine the value of the optical band gap, which was 1.78 eV which confirms the ionic nature of the $Sb_2S_3$ material.

The influence of the deposition temperature and the temperature of subsequent annealing in the $N_2$-S atmosphere on the properties of $Sb_2S_3$ thin films deposited by spraying [64] was investigated. The films were applied to substrates of which temperature varied from 200°C to 350°C. Regardless of the substrate temperature, the sprayed films were amorphous, but after annealing at $300^0$C they turned into polycrystalline. The properties of the annealed films such as crystallite size, deformation, grain size, refractive index and stoichiometry depend on the deposition temperature.

$Sb_2S_3$ thin films were obtained by high-frequency magnetron sputtering and their characteristics were studied before and after heat treatment [65]. The films crystallized into a rhombic structure after heat treatment at 300°C in the medium of $N_2$/S determined by X-ray and Raman spectroscopy. Elemental analysis by EDXS showed a slight excess of sulfur in the films. Optical properties and electronic transitions between zones were determined by Spectroscopic Ellipsometry.

The structural, optical and electrical properties of sprayed $Sb_2S_3$ films grown by simple thermal evaporation were studied [66]. The films were annealed at 300°C in various atmospheres: vacuum, sulfur vapors, air and nitrogen. Their structural, morphological, electrical and optical properties were analyzed investigated. The values of some important parameters of the film, such as absorption coefficient and band gap energy, are determined from the transmission spectra. Polycrystalline films of antimony trisulfide had high absorption coefficients in the range $10^4$-$10^5$ $cm^{-1}$, and the direct optical band gap was 1.64-1.71 eV.

$Sb_2S_3$ films were obtained on $LiNbO_3$ and glass substrates by vapor deposition. The structure of these films was amorphous, but after annealing in a sulfur atmosphere, they turned into polycrystalline form. The dependence of the optical and structural properties of the films on the annealing temperature was studied. A sharp change in optical transmission, energy bandgap, refractive index, size of the crystallites and other properties was observed at a temperature of about 200°C [67].

$Sb_2S_3$ thin films were sprayed onto amorphous glass substrates using glacial acetic acid as a non-aqueous solvent [68]. The films were prepared by spraying $SbCl_3$ and $CS(NH_2)_2$ dissolved in equimolar amount in acetic acid onto the glass substrates heated up to the temperature of 250°C in a solution concentration of 0.1 M. The spray rate was maintained at 12 $cm^3$/min during film deposition. The films were deposited with different volume ratios of Sb:S in solution: 1:9, 2:8, 3:7, 4:6, 5:5, 6:4, 7:3, 8:2 and 9:1. Their structural, optical and electrical properties were investigated.

$Sb_2S_3$ and $Sb_2Se_3$ thin films were obtained by spray pyrolysis from aqueous and non-aqueous media. Thin films of $Sb_2S_3$ were prepared from the aqueous electrolyte using equimolar solutions of antimony trichloride and thioacetamide in corresponding volumes to achieve a 2:3 ratio of Sb:S. Tartaric acid, which forms a strong complex with antimony and slows the formation of sulfide deposits between antimony trichloride ($SbCl_3$) and thioacetamide ($CH_3CSNH_2$), was used as a complexing agent. The tartaric acid concentration was maintained at the optimal level of 0.5 M. For the non-aqueous electrolyte, equimolar (0.1 M) solutions of $SbCl_3$ and $CS(NH_2)_2$ were mixed in volumes conforming to obtaining a 2:3 ratio of Sb:S in acetic acid (glacial). The mixed solutions were left for about 12 hours until the yellowish precipitate disappeared and a clear solution was obtained. Films were prepared by spraying 20 $cm^3$ of solutions onto hot glass substrates maintained at 250°C optimal temperature. The deposited films were dark brown, uniform and adhered well to glass substrates. Studies show that films obtained from aqueous media are amorphous, while films obtained from non-aqueous media are polycrystalline [69]. It was revealed that the $Sb_2S_3$ films have n-type conductivity, whereas $Sb_2Se_3$ films having p-type conductivity independently of the synthesis medium, moreover all of the resulting thin films, are photoactive.

Thin films of antimony ($Sb_2S_3$) were grown on the Mo-coated glass substrate by evaporation of metal Sb with subsequent annealing in an $N_2/H_2S$ medium. It was found that, the metal layer Sb is not completely sulfonated at the annealing temperature of 320°C, and at a temperature above 450 ° C, the loss of $Sb_2S_3$ occurs. Films obtained at an annealing temperature of 400°C [70] had improved morphology and phase structure.

The authors of [71] found that co-evaporation of sulfur or antimony with $Sb_2S_3$ is capable of generating $Sb_2S_3$ rich in sulfur or antimony. Studies show that the film enriched in sulfur $Sb_2S_3$ is effective at converting energy, while the film enriched in antimony significantly reduces the performance of the device. The final energy conversion efficiency reaches 5.8% due to the optimization of $Sb_2S_3$ films with a high amount of sulfur, which is the highest evaluating parameter of the thermal evaporation efficiency obtained on the $Sb_2S_3$.

$Sb_2S_3$ thin films were obtained by depositing the $Sb_2S_3$ powder on glass substrates by evaporation at room temperature under pressure. The composition of the films and the effect of vacuum annealing on their structure were determined. The deposited films were amorphous, whereas the annealed films had an orthorhombic polycrystalline structure [72].

$Sb_2S_3$ amorphous thin films were prepared by thermal evaporation of the corresponding powder on cleaned glass substrates heated to 300-473K. It was found that as the substrate temperature increased, the band gap decreased from 1.67 eV at 300K to 1.48 eV at 473K [73].

In work [74], the vacuum sputtering method was used to obtain high-efficient $Sb_2S_3$

solar cells. Antimony (III) chloride ($SbCl_3$) and thiourea (TU) are used as initial materials which are dissolved in 2-methoxyethanol (2-ME) for the synthesis of $Sb_2S_3$. Studies show that this method makes it possible to produce absorbent materials of $Sb_2S_3$ with a high degree of crystallinity and phase purity, which contribute to increasing the performance of the device. When using $TiO_2$ nanorod arrays as the electron extraction material for constructing solar cells, the device efficiency increased from 4.15% to 6.78%, which is one of the most important parameters of efficiencies in all kinds of $Sb_2S_3$, $Sb_2(S,Se)_3$ and $Sb_2Se_3$-based solar cells.

Equimolar solutions of antimony trichloride and thioacetamide were used in volumes equivalent to obtaining a 2:3 ratio of Sb:S to prepare the films. Oxalic acid was used as a complexing agent. 20 $cm^3$ of 2M oxalic acid was mixed with 100 $cm^3$ of 0.1M antimony trichloride. This inhibits the formation of a sulfide deposit occurring between antimony trichloride and thioacetamide. 150 $cm^3$ of a 0.1M solution of thioacetamide was mixed with a complexing solution of antimony trichloride. The mixed solution was immediately sprayed onto hot glass substrates (300°C). The spray rate was 14 $cm^3$/min; and the air was used to spray the solution. The effect of the substrate temperature and solution concentration on the structure, optical and electrical properties of the films was studied. The films are amorphous and have semiconductor properties [75].

The effect of thermal annealing on the structure and optical properties of antimony trisulfide ($Sb_2S_3$) thin films deposited on a glass substrate by thermal evaporation in a vacuum was studied. Structural studies performed using X-ray diffraction (XRD) and atomic force microscopy (AFM) showed that $Sb_2S_3$ films had an amorphous structure, which became polycrystalline after annealing at a temperature of 500K [76].

## Chemical deposition methods

$Sb_2S_3$ thin films were prepared by chemical deposition method on amorphous glass substrates at room temperature using antimony chloride ($SbCl_3$) and sodium thiosulfate ($Na_2S_2O_3$. $5H_2O$) [77]. X-ray diffraction showed that the structure of $Sb_2S_3$ thin film changes from amorphous to polycrystalline after annealing at 350°C for 1 hour in a nitrogen atmosphere.

In [78], $Sb_2S_3$ thin films were also deposited on glass substrates at room temperature by chemical deposition. The reaction bath contained 20 ml of 0.1M antimony trichloride, 20 ml of 0.1M sodium thiosulfate and 32 ml of 0.1M ethylenediaminetetraacetic acid (EDTA), which was used as a complexing agent. Optical studies have shown a decrease in the band gap by 0.15 eV and an increase in the photoconductive properties of the films after annealing in air at a temperature of 473 K. The effects of the film thickness on the absorption coefficient, reflectance, refractive index, extinction coefficient, real and imaginary parts of the dielectric permittivity were estimated in the wavelength range of 30–900 nm. It found that the reflection coefficient, adsorption coefficient, real part of the dielectric permittivity, and refractive index decrease with increasing film thickness, while the imaginary part of the dielectric permittivity increases. [79].

The authors of [80] obtained thin films of $Sb_2S_3$ on a glass substrate by chemical deposition. The films were prepared in the reaction bath at temperatures of 283, 303, 323, and 243 K in the constant-time deposition. At high temperatures, dissociation is stronger and gives higher concentrations of $Sb^{3+}$ and $S^{2-}$ ions in the reaction bath, which increases the deposition rate. Also, an increase in the deposition temperature leads to the transition of the film structure from amorphous to polycrystalline. Optical studies showed that the films have direct allowed transitions in the range of 1.86–2.30 eV depending on the film thickness. It was found that the activation energy decreases from 0.67 to 0.48 eV at low and 0 temperatures.

Thin films of $Sb_2S_3$ were obtained by chemical deposition and annealed at temperatures of 373 and 473 K [81]. $SbCl_3$ and $Na_2S_2O_3$ were used as initial substances and dissolved in 50 ml of acetone. The absorption and transmission spectra were recorded in the wavelength range of 300-900 nm and the nature of the electronic transitions was determined. It was established that these films have a direct allowed transition with an optical band gap of 1.72, 1.76, and 1.82 eV before and after annealing, respectively. We also measured the extinction coefficient, refractive index, real and imaginary parts of the dielectric permittivity before and after annealing.

Thin films of antimony sulfide were obtained by chemical deposition in a bath, which was then subjected to thermal annealing in a nitrogen atmosphere [82]. The sorbed (fixed), plasma-treated and thermally annealed antimony sulfide was studied by X-ray diffraction (XRD), energy dispersive X-ray spectroscopy, scanning electron microscopy, atomic force microscopy, ultraviolet radiation; and electrical measurements were also carried out. X-ray diffraction studies showed that the crystallinity was improved in both states. Studies by atomic force microscopy have shown that the change in the morphology of deposits depends on their treatment after deposition. Also, after treatment, the optical band gap of the films ($E_g$) decreased (from 2.36 to 1.75 eV) due to the improvement in grain sizes. The electrical resistivity of $Sb_2S_3$ thin films decreased from $10^8$ to $10^6$ $\Omega\cdot$cm after plasma treatment.

It was established in [83] that thicker films of $Sb_2S_3$ might be obtained with a longer and multiple chemical deposition. The authors added a small amount of ethylenediaminetetraacetic acid (EDTA) to the traditional chemical reagents used in the deposition of $Sb_2S_3$ films. The effect of the concentration of EDTA and $Na_2S_2O_3$, bath temperature and deposition time on the composition and quality of deposits was studied. It became possible to obtain homogeneous $Sb_2S_3$ thin films of high quality with a thickness of more than 1 μm in a short deposition time (3 hours) by optimizing these conditions. The films were subjected to annealing to improve their crystallinity and had an orthorhombic crystal structure with lattice parameters *a = 1.142 nm, b = 0.381 nm, c = 1.124* nm and a band gap in the direct optical range was 1.66 eV.

Semiconductor films of antimony sulfide $Sb_2S_3$ were synthesized by chemical deposition on a glass substrate from glycine baths [84, 85]. The film thickness was about 0.62 nm. The deposited films were uniform and had good adhesion to glass substrates. The films had a polycrystalline nature, and the band gap determined from the optical absorption spectra was 2.10 eV. An analysis of the composition of the films showed that they almost corresponded to the stoichiometric composition. 10 ml (0.2M) $SbCl_3$, 4 ml (1 M) malonic acid, and 15 ml (0.2 M) sodium thiosulfate was added to a 50 ml beaker to carry out the deposition process. The total volume was adjusted to 40 ml with bidistilled water. In this case, the pH of the reaction mixture is 4.56. The beaker was kept in an ice bath. The temperature of the reaction bath slowly rises to 298 K. After 3 h, the glasses are removed, washed several times with bidistilled water, and stored in desiccators. The deposited $Sb_2S_3$ thin film was dark red.

The authors of [86–88] obtained thin films of $Sb_2S_3$ on a glass substrate using the successive ionic layer adsorption and reaction (SILAR) method with different time cycles. The synthesis was carried out in the solution containing $SbCl_3$ and $Na_2S_2O_3$ in ethylene glycol at room temperature, and the thickness of obtained films was in the range of 0.145 μm, 0.216 μm, and 0.239 μm. The photoluminescent spectra of the deposited $Sb_2S_3$ thin films show a strong blue emission peak at 460 nm. The obtained $Sb_2S_3$ films consist of uniformly distributed $Sb_2S_3$ clusters crystallized at a relatively low temperature (250°C) from the bottom to the top of ZnO nanowires. In addition, it has high purity, as only a very slight phase of senarmontite-$Sb_2O_3$ is detected by Raman scattering spectroscopy, and has an appropriate band gap of 1.74 eV obtained from the Tauc plot within the two-pass analysis. These results show the high potential of the SILAR method for the formation of heterostructures of ZnO core–shell nanowires with high uniformity at moderate temperatures, as well as its advantages in comparison with the most widely used chemical bath deposition method [89].

The authors of [90] proposed a centrifuged deposition method to obtain homogeneous and high-quality $Sb_2S_3$ films, which eliminates the formation of antimony oxides, reduces the deposition time, and makes it possible to control the film thickness. The influence of the process conditions (solution composition and concentration of the components, multiplicity of coverings, and rotation speed of the centrifuge) on the morphology, chemical composition, and crystal structure of $Sb_2S_3$ thin films was studied. Flat solar cells based on $Sb_2S_3$ thin films were prepared and their photovoltaic properties were studied to estimate these thin films.

A thin film of antimony sulfide was deposited on a glass substrate by chemical deposition in a bath at room temperature [91]. $SbCl_3$ and $Na_2S_2O_3$ dissolved in acetone were taken as a source of antimony and sulfur. According to the absorption and transmission spectra determined using the Unico UV-2102 PC spectrophotometer, the band gap was determined, which ranged from 1.60 to 2.30 eV.

Antimony sulfide films were obtained by growth technique from solution and doped with nickel impurities [92]. The films were then subjected to annealing at temperatures from 50 to 200°C for 1 hour. Studies conducted by X-ray diffractometry and UV spectroscopy made it possible to reveal the optical constants of the obtained films. The results of the structural analysis show that the obtained films are mainly amorphous and exhibit a polycrystalline form at the annealing temperature of 150°C. Optical measurements show that the optical absorption coefficient was > $10^4$ $cm^{-1}$, the energy band gap was direct in the range from 2.26 eV to 2.52 eV values.

Thin layers of $Sb_2S_3$ were obtained from a non-aqueous electrolyte at room temperature. The deposition was carried out using a 0.1 M solution of antimony trichloride ($SbCl_3$) and thioacetamide ($CH_3CSNH_2$). The films were recommended for use in super condensers as an active material. The composition, morphology, and structure of the obtained films were studied. The electrochemical characteristics were evaluated using the methods of cyclic voltammetry, galvanostatic charge-discharge, and electrochemical impedance spectroscopy [93].

High-quality semiconductor thin films of antimony sulfide ($Sb_2S_3$) were directly produced on indium tin oxide (ITO) substrates by a one-step hydrothermal reaction without any chelating reagents. $KSbC_4H_4O_7$ and $Na_2S_2O_3$ were used as a precursor for Sb and S, respectively [94]. The obtained $Sb_2S_3$ films had a relatively ideal S/Sb atomic ratio and a compact surface. The $Sb_2S_3$ film annealed at 450ºC showed improved optical and electrical characteristics. The optical band gap of the films was estimated from the optical absorption spectra; the band gap values were in the range of 1.7–2.1 eV. All rapidly thermally treated samples showed a photoconductive response reaction. The crystallinity and morphology of the films varied by changing the temperature and time of rapid heat treatment [95].

Semiconductor $Sb_2S_3$ thin films were chemically deposited onto $SnO_2$:(F)/glass substrates from an aqueous medium at low temperatures (40–70°C) [96]. The selected chemical bath was slightly acidic (pH = 3.8). The formation of antimony sulfide films can be explained by various mechanisms depending on the dissociation of thiosulfate ions. In this work, the dissociation of thiosulfate ions occurs according to the reaction in the acidic solution:

$$S_2O_3^{2-} + H^+ \rightarrow S + HSO_3^- \qquad (1)$$

Since thiosulfate is a reducing agent, it can act as an electron donor and reduce S to $S^{2-}$. Thiosulfate forms a very strong complex $Sb_2(S_2O_3)_3$ with the antimony ion ($Sb^{2+}$), which is hydrolyzed to form $Sb_2S_3$ according to the following chemical reaction:

$$Sb_2(S_2O_3)_3 + 3H^+ + 6e^- \rightarrow Sb_2S_3 + 3HSO_3^- \ (2)$$

or

$$2Sb^{3+} + 3S^{2-} \rightarrow Sb_2S_3 \qquad (3)$$

$Sb_2S_3$ film begins to deposit on the substrate when the ionic product (IP) of the $Sb^{3+}$ and $S^{2-}$ ions formed as a result of reactions in the bath exceeds the solubility product ($K_D = 10^{-92.77}$) of $Sb_2S_3$. The obtained films showed good optical properties with a direct band gap of about 2.30 eV.

The review article [97] describes in detail the methods of chemical deposition of thin films of metal chalcogenides of good quality. Their structural, optical, electrical and other properties are described. Moreover, the theoretical prerequisites necessary for the chemical deposition of thin films are also discussed.

$Sb_2S_3$ thin films were chemically deposited at 40°C from a mixture of potassium and antimony tartrates, triethanolamine, ammonia, and thioacetamide (TA) and at 1–10°C from a mixture of antimony trichloride and thiosulfate (TS) [98]. After heat treatment of the films from 250 to 300°C, they became photoconductive.

In [99–106], $Sb_2S_3$ thin films were also obtained by chemical deposition. $Sb_2S_3$ films were deposited on a glass substrate using aerosol-assisted chemical vapor deposition [99], while thin $Sb_2S_3$ suspensions were deposited from a non-aqueous medium of glacial acetic acid at room temperature (27°C) [100]. $Sb_2S_3$ thin films were deposited on glass substrates at 300 K by chemical deposition and annealed at various temperatures [101]. The annealed film got a thickness of 0.440 μm (453 K) and 0.691 μm (473 K). Optical measurements show that the observed direct optical transitions slightly decline from 2.20 eV to 1.60 eV due to the annealing temperature.

The films have high absorption in the UV region, over 90%. $Sb_2S_3$ thin films with a thickness of 600 nm were obtained by chemical deposition. $CuSbS_2$ films were obtained based on them by heating glass /$Sb_2S_3$/Cu layers in order to use them as an absorber material in photovoltaic structures: glass / $SnO_2$: F / n-CdS / p-$CuSbS_2$/C/Ag [102]. The optical band gap of $CuSbS_2$ thin films was 1.55 eV, while the films were photoconductive.

Crystallization of $Sb_2O_3$ thin films by systematic annealing includes the intermediate formation of the metallic Sb phase and very often the cubic senarmonite $Sb_2O_3$ phase; moreover both of them disappear before the formation of the $Sb_2S_3$ stibnite phase. Combined in situ X-ray scattering of chemically deposited $Sb_2S_3$ thin films was performed at a very low power of laser with diffraction in a wide range of temperatures and annealing times in an $N_2$ atmosphere [103]. Compact thin films of $Sb_2S_3$ with a thickness of 150 nm crystallize in the range from 240 to 270°C; below the commonly used annealing temperature of 300°C. $Sb_2S_3$ thin films crystallized at the optimal annealing temperature of 270°C consist of dense crystallites with a typical size of a few tens of nanometers that represents a great interest for their integration into solar cells.

In [104], the results of the thin film deposition of antimony sulfide and selenide from chemical baths containing $SbCl_3$ and a source of sulfide or selenide ions in the presence of ligands that form soluble complexes with antimony are presented. The deposited films have an amorphous structure; however, after annealing in the nitrogen atmosphere at a temperature of about 350°C, clear peaks confirming the formation of antimony sulfide and selenide appeared on the X-ray patterns. This work also deals with preparing the new thin-film materials by annealing multilayer thin films in the presence of antimony chalcogenide films that would make it possible to prepare thin-film semiconductors covering a wide range of structural, electrical, and optical properties for photonic applications [104].

Antimony sulfide ($Sb_2S_3$) thin films were prepared by laser-assisted chemical bath deposition (LACBD) onto glass substrates from a solution containing antimony chloride, acetone, and sodium thiosulfate [105]. The chemical deposition and irradiation conditions varied. The results showed that LACBD is an efficient method for synthesizing $Sb_2S_3$ thin films suitable for optoelectronic devices. The obtained films were irradiated with a continuous wave laser beam of 532 nm wavelength under various conditions in an air atmosphere [106]. X-ray diffraction analysis showed that under the action of laser radiation, the structure of $Sb_2S_3$ thin films was transformed from amorphous to polycrystalline.

The chemical deposition of thin Mn-doped $Sb_2S_3$ films was carried out by authors of [107] for the first time from a solution containing antimony chloride ($SbCl_3$), manganese acetate (Mn $(CH_3COO)_2 \cdot 2H_2O$), and sodium thiosulfate ($Na_2S_2O_3 \cdot 5H_2O$) at room temperature. Their structural, optical, morphological, magnetic and photoelectric properties were studied. The results showed that the range of the spectral response of Mn-doped $Sb_2S_3$ films is wider than that of undoped films. The authors suggest that the introduction of dope-additives during the synthesis of $Sb_2S_3$ can serve as an effective means of improving the characteristics of solar cells.

$Sb_2S_3$ thin films were obtained on glass substrates from a chemical bath containing $SbCl_3$ and $Na_2S_2O_3$ salts at room temperature (27°C). A thin carbon film was deposited on the $Sb_2S_3$ film by vacuum arc evaporation, and then the $Sb_2S_3$–C layer was subjected to heating at 300°C for 30 min in the nitrogen atmosphere or in the low vacuum [108]. The resistivity value of $Sb_2S_3$ thin films decreased from 108 Ω for the undoped state to 102 Ω for doped thin films, a change in their electrical properties was observed in this case. The electrical resistivity of $Sb_2S_3$ can be controlled by changing the carbon content of the deposits (w/w %) which makes them suitable for various optoelectronic setups.

The effect of dyestuff concentration on the morphological and optical properties of antimony sulfide ($Sb_2S_3$) thin films deposited on a glass substrate by chemical deposition was studied [109]. The concentration of the dyestuffs varied, while the other deposition conditions remained constant. The analysis showed that the sensitization of antimony sulfide thin films improved their optical properties by increasing the transmittance factor and band gap.

## Electrochemical deposition methods

The electrochemical deposition method for thin films has some interesting advantages over other methods, such as: 1) ease of implementation; 2) easy of obtaining non-crystalline phase; 3) effortless control of alloy composition; 4) ease of process control; 5) possibility of obtaining a multilayer film on the cheap [110].

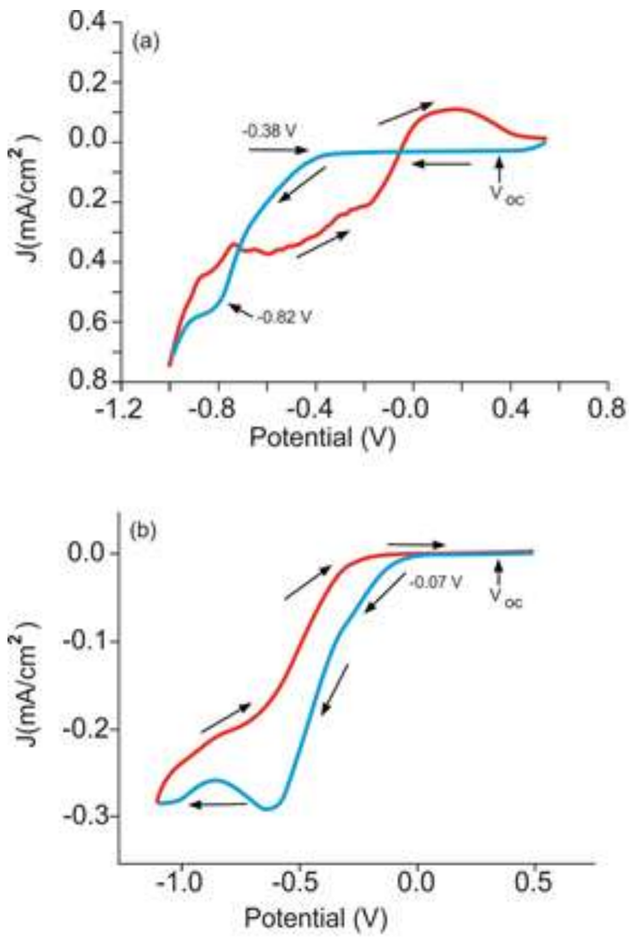

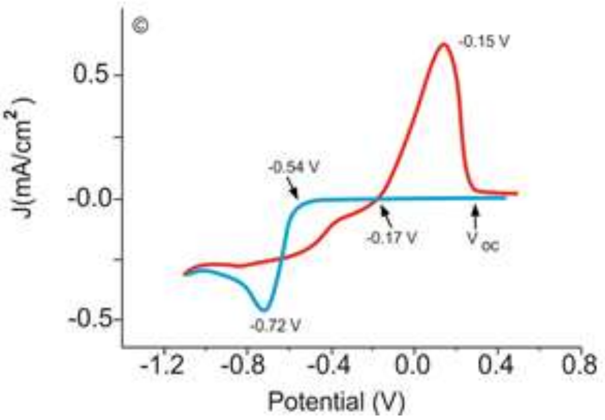


**Fig. 1.** Cyclic voltammograms of deposition: (a) antimony 1,5 mM $SbCl_3$; (b) sulfur 18 mM $Na_2S_2O_3$; (c) antimony with sulfur 1,5 mM $SbCl_3$ + 18 mM $Na_2S_2O_3$, pH of the electrolyte 2,5–3, t = 25°C, υ =10 mV/s [111].

In [111], antimony sulfide was obtained from aqueous solutions containing $SbCl_3$ and $Na_2S_2O_3$ by pulsed electrodeposition on fluorine-doped glass substrates coated with $SnO_2$. The crystal structure of the films was characterized by X-ray diffraction, Raman spectroscopy, and TEM analysis. The deposited films were amorphous, and after annealing in a nitrogen/sulfur atmosphere at a temperature of 250°C for 30 min, the films crystallized, and the results of X-ray phase studies showed that the films comply to $Sb_2S_3$ stibnite (the X-ray diffraction pattern coincides with that of $Sb_2S_3$ antimonite (JCPDS 6-0474).

Atomic force microscopy images showed that $Sb_2S_3$ films have uniformly distributed grains on the surface, whereas grain agglomeration occurs during annealing. The optical band gap for films after deposition and after annealing at 300°C calculated from studies of the transmission and reflection coefficients was 2.2 and 1.65 eV, respectively. The cyclic voltammetric curves were taken for individual components and for co-deposition under the same conditions to determine the deposition potential of $Sb_2S_3$ thin films [111].

Figure 1 (a) shows cyclic voltammograms in 1.5 mM $SbCl_3$ solution. The value of the current at the beginning of the recording of the curves remained almost equal to zero relatives to the silver chloride electrode up to a potential value of 0.38 V. When the potential is shifted to the negative side, a sharply defined cathode peak appears at a potential of 0.82 V, and deposition of metallic Sb occurs according to the reaction (4):

$$Sb^{3+} + 3e^- \rightarrow Sb^0 \qquad (4)$$

Hydrogen evolution reaction is observed with a further shift of the potential to the negative side. Sb deposit dissolves in the reverse of the curve (red line). Polarization studies show that the deposition of Sb from 1.5 mM $SbCl_3$ occurs in the potential range of -0.38 ÷ - 0.84 V according to HSE. Figure 1(b) shows polarization curves of S deposition from 18 mM $Na_2S_2O_3$ solution. At a potential of about 0.07 V, the current sharply increases due to the reduction of thiosulfate to sulfur according to the reaction (5):

$$S_2O_3^{2-} + 6H^+ + 4e^- \rightarrow 2S + 3H_2 \qquad (5)$$

There is a possibility that the adsorbed sulfur will be reduced to $H_2S$ in accordance with the reaction (6).

$$S + 2H^+ + 2e^- \rightarrow H_2S \quad (6)$$

The absence of an anodic peak in the reverse of the curve may be due to the fact that either the adsorbed sulfur was reduced to $H_2S$ during the cathode process, or the deposited material did not dissolve in the electrolyte at the applied anodic potentials. The co-deposition voltammograms from the mixture of 1.5 mM $SbCl_3$ and 18 mM $Na_2S_2O_3$ give the co-deposition potential of $Sb_2S_3$ (Fig. 1(c)). The electric current during the direct route of the curve remained almost zero up to the potential of -0.54 V relative to the silver chloride electrode. A rapid increase in the cathode current is observed at the potential value of -0.54 V, which may be associated with the formation of antimony sulfide according to reactions (7) or (8):

$$2Sb^{3+} + 3S + 6e \rightarrow Sb_2S_3 \quad (7)$$
$$2Sb^{3+} + 3H_2S \rightarrow Sb_2S_3 + 6H^+ \quad (8)$$

$Bi_2S_3$, $Sb_2S_3$, and $As_2S_3$ thin films were obtained from aqueous acidic baths by electrodeposition using $Na_2S_2O_3$ as a sulfide source [112]. Thin, homogeneous films well adhered to the surface of the substrate were deposited from the bath with the EDTA complexing agent. The electrodeposition potentials were determined by recording polarization curves. The structural and optical properties of the films were studied. The X-ray diffraction pattern showed that the films have a polycrystalline structure. The values of the optical band gap energy for $Bi_2S_3$, $Sb_2S_3$ and $As_2S_3$ are 1.58 eV, 1.74 eV, and 2.35 eV, respectively.

The composition dependence of the electrolysis conditions of $Sb_2S_3$ thin semiconductor films electrodeposited from an aqueous electrolyte containing SbOCl and $Na_2SO_3$ was studied in the galvanostatic mode [113]. The range of potentials at which antimony deposits together with sulfur is determined to study the kinetics of polarization by the potentiodynamic method. Figure 2a shows the cyclic polarization curve of the co-deposition process of antimony with sulfur on the Pt electrode.

The curve was recorded in the potential range of 1.0 ÷–0.85V. It can be seen that the electro-reduction of sulfite ions occurs according to the reaction starting from the stationary potential of 0.3 V and progressing up to the potential of –0.5 V:

$$HSO_3^- + 5H^+ + 4e^- \rightarrow S + 3H_2O$$

Further, sulfur is deeply reduced to sulfide ions starting from –0.5 and continuing up to –0.7 V according to the following reaction:

$$S + 2e \rightarrow S^{2-}$$

The obtained sulfide ions react with antimony ions after a potential of –0.7 V and are deposited on the electrode surface in the form of Sb–S:

$$2Sb^{3+} + 3S^{2-} \rightarrow Sb_2S_3$$

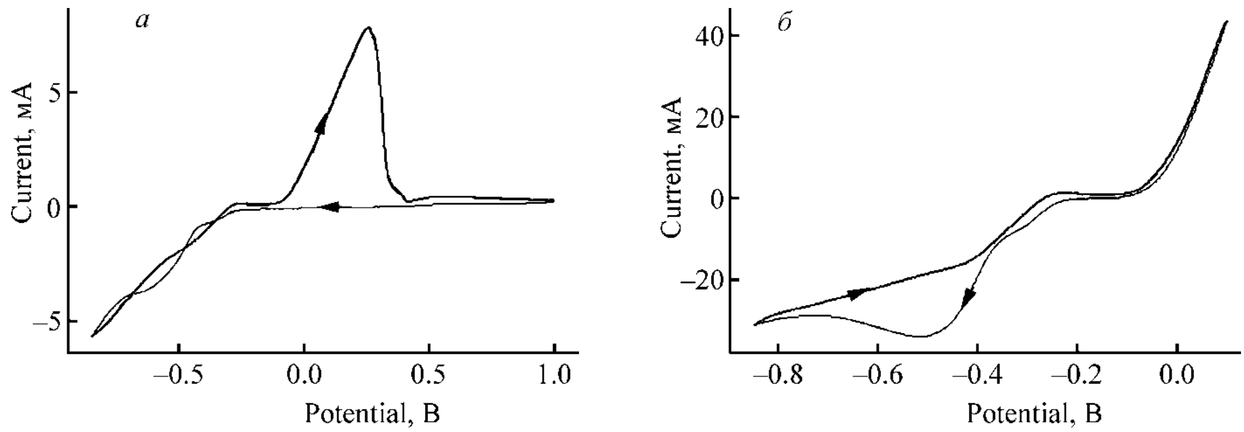


**Fig. 2.** Cyclic polarization curve of electrodeposition of $Sb_2S_3$ thin films on (a) Pt and (b) Ni electrodes, electrolyte (M): 0.06 SbOCl + 0.04 $Na_2SO_3$ + 0.007 $C_4H_6O_6$, T = 298 K, $E_V$ = 0.03 $V \cdot s^{-1}$ [113]

The co-electrodeposition of antimony with sulfur was also studied on a porous nickel electrode. As is seen from Fig. 2b, as compared with the platinum electrode, electrodeposition proceeds according to the same mechanism, only, there is an anode maximum in Fig. 2a, while there is a cathode maximum in 2b. The cathodic peaks are observed at a potential of –0.5 V on both electrodes. It is shown that the content of antimony in the obtained films increases with an increase in the SbOCl concentration and electrolysis time. As the electrolyte temperature, current density, and $Na_2SO_3$ concentration increase, the content of antimony in thin films decreases.

The optimal electrolyte composition and the electrochemical deposition mode were also established for obtaining thin films of the chemical compound $Sb_2S_3$ with a composition close to stoichiometry. The optimal condition for the deposition of thin films with 3–5 mm thickness is as follows: 0.06 M SbOCl + 0.04 M $Na_2SO_3$ + 0.007 M $C_4H_6O_6$ (tartaric acid), T = 298–308 K, current density 5 mA $cm^{-2}$, the electrolysis time is 150 min. The obtained X-ray diffraction patterns indicate that, using this optimal condition, $Sb_2S$ thin films are deposited in a crystallite size of ~80–100 nm [113].

Thin films of polyaniline (PAni) containing $Sb_2S_3$ were obtained by electrodeposition. Polymer films are polymer-modified electrodes with metal particles embedded in thin films either during the formation of the film or during electrodeposition on polymer films [114]. Polymer-semiconductor composites have not only the characteristic flexibility and manufacturability of the polymer, but also the mechanical strength and hardness of semiconductor compounds. The deposition was carried out at three different concentrations of PAni. The morphology of the doped films changes with the addition of PAni, and the X-ray diffraction pattern indicates the polycrystalline nature of all films. In addition, it was found that the size of the crystallites increases with an increase in the concentration of PAni. The conductivity of samples obtained at various concentrations of PAni was studied as a function of temperature.

The authors used $Na_3[SbS_4] \cdot 9H_2O$ as the only one initial component [115] for the electrodeposition of $Sb_2S_3$ from an aqueous electrolyte at pH 9.1. They represented the electrochemistry of the $[SbS_4]^{3-}$ anion and the observed redox processes for the deposited $Sb_2S_3$ film. The amorphous $Sb_2S_3$ film can be deposited by anodic electrodeposition on glassy carbon, and in addition, it is possible to avoid the formation of the by-product accompanying this deposition by using a suitable pulsed deposition method. Raman spectroscopy and X-ray analyses have shown that crystalline $Sb_2S_3$ films of high quality are formed during annealing. $Sb_2S_3$ crystalline films were tested for Resistive Random-Access Memory applications; and it was shown that $Sb_2S_3$ crystalline films exhibit typical bipolar resistive switching behavior. The resistance ratio between the high resistance state and the low resistance state is about one order of magnitude at 1.5 V, which is sufficient for memory applications. A resistive switching mechanism was also proposed in the paper.

A comparative analysis of the reviewed methods for obtaining $Sb_2S_3$ thin films allows us to draw the following conclusions:

- The use of high temperatures in a thermal deposition may cause deformation or damage to the deposited $Sb_2S_3$ thin films. In addition, high temperatures can lead to the spreading of the layers, which can adversely affect the structure and properties of the films. Also, during thermal deposition, the layers may be inhomogeneous in thickness and in composition. This is due to the diffusion and condensation processes during deposition, which can lead to an uneven distribution of the composition over the film thickness.

- It is more difficult to control the quality of the resulting layers in chemical deposition. Along with this, chemical deposition methods can be prone to contamination due to the using reagents and solutions. Uncontrolled impurities can lead to defects in the structure or deterioration of the properties of the obtained films. Also, during the chemical deposition of $Sb_2S_3$ thin films from aqueous, non-aqueous, and complex solutions, the obtained deposits usually have an amorphous structure, which transforms into a polycrystalline one under the influence of temperature in an air or nitrogen atmosphere, or under the influence of the laser. It should be noted that it is impossible to obtain thin films of the desired thickness by chemical deposition. This is due to the fact that after the deposition of the monolayer, the surface of the substrate is passivated and, by reason of this, further co-deposition does not occur on the surface of the substrate.

As compared to the above methods, the electrochemical deposition method of $Sb_2S_3$ thin films is a powerful tool for controlled formation of the coatings, but requires careful optimization of parameters and consideration of limitations to achieve the desired results. Also, this method allows for achieving uniform coating on complex shapes and surfaces. In addition, the adhesion of films obtained with this method is relatively high. Electrochemical deposition of thin films is economically advantageous, since this method does not require sophisticated equipment, high temperature, high pressure, and the consumption of used raw materials is very low.

## Study of properties of $Sb_2S_3$ thin films

One of the intermediate steps in the organo-colloidal synthesis of crystalline $Sb_2S_3$ is the synthesis of spherical amorphous $Sb_2S_3$. The electronic and photoelectric properties of thin amorphous and polycrystalline $Sb_2S_3$ films were studied to prove that the synthesized semiconductor is able to serve as an absorbing material in solar devices. Optical studies showed that the direct band gap was 1.65 eV and the two direct allowed transitions were 1.57 and 1.91 eV for polycrystalline and amorphous thin films, respectively [116].

The study of the effect of Ag doping on the structural, optical, and electrical properties of thin $Sb_2S_3$ films shows that Ag insertion occurred in the $Sb_2S_3$ lattice forming more uniform and dense films as compared to undoped films [117]. In addition, the band gap of $Sb_2S_3$ got narrower from 1.75 to 1.66 eV, which led to a redshift of the absorption onset from 750 to 800 nm. It found that the crystallization temperature of $Sb_2S_3$ can be controlled by Ag-doping; and the temperature was reduced by 100 K by doping with 12 at.% Ag. In general, an increase in the annealing temperature accelerates the crystallization process. However, the electric field contributed to the dissolution of Ag and an increase in the silver content in $Sb_2S_3$, which led to the formation of holes in the amorphous structure. Holes accelerated the nucleation process and, consequently, reduced the time required for complete crystallization [118, 119].

The authors of [120] revealed that doping of $Sb_2S_3$ films with 8.6% copper occurred on the surface and boundaries of the $Sb_2S_3$ grains. Here, the copper mostly bonded with sulfur, which increased the number of sulfur vacancies thereby causing an increased concentration of the carrier, better crystallinity, increased grain size, and reduced phase defects of $Sb_2O_3$. As a result, the carrier concentration and band gap were significantly increased from $6.28 \times 10^9$ to $6.06 \times 10^{10}$ $cm^{-3}$ and from 1.65 to 1.83 eV, respectively. Consequently, the Fermi level rises indicating that Cu is n-type doping for $Sb_2S_3$. This photoanode showed an efficiency factor of 1.13%, while the undoped dummy cell showed an efficiency factor of only 0.86%.

The work [121] reported on the efficiency factor of solar cells using mesoporous $TiO_2$ films sensitized by stibnite ($Sb_2S_3$) quantum dots. The authors carried out atomic studies of the interface between $TiO_2$ and $Sb_2S_3$.

The thermoelectric behavior of antimony trisulfide ($Sb_2S_3$) thin film was investigated based on the analysis of the energy band structure, calculation of the quality factor (energy factor) and Boltzmann transport properties using thermodynamic modeling. The results show that $Sb_2S_3$ exhibits thermoelectric features at temperatures ≥ 600K. This means that, under appropriate doping conditions, antimony trisulfide thin films can be used in the exhaust heat recovery system of exhaust gases. Typically, a value known as the quality index (ZT) is found to determine the thermoelectric behavior of the material. It is related to the Seebeck coefficient S, electrical conductivity σ and thermal conductivity according to the equation (9):

$$ZT=\frac{S^2 \sigma T}{\kappa} \qquad (9)$$

In equation (9), S is the thermo-emf (electromotive force) or Seebeck coefficient, σ is the electrical conductivity, and κ is the thermal conductivity [122, 123]. It is seen from the equation that, a high value of the Seebeck coefficient (S) and electrical conductivity (σ) is required to increase the value of ZT, and the value of thermal conductivity (κ) must be minimal.

In order to improve the poor absorption of visible light and the low quantum efficiency of $TiO_2$, $TiO_2/Sb_2S_3$ heterojunction (photoanode) was synthesized [124], where a higher photocurrent density of 0.33 $mAcm^{-2}$ (measured at 1.23 V compared to a reversible hydrogen electrode) was obtained in 0.5 M aqueous solution of $Na_2SO_4$ under general lighting. This successful combination of two n-type semiconductors as a photocatalyst to achieve efficient water oxidation provides a conceptual layout for developing a composite with additional optical and electrical properties.

In [125], the hydrothermal method failed to uniformly deposit $Sb_2S_3$ films on the $TiO_2$ substrate. Therefore, for the first time, a reactive ion etching (RIE) treatment was developed for the $TiO_2$ surface to activate it for the subsequent deposition of $Sb_2S_3$. Based on this strategy, the obtained $Sb_2S_3$ film has much in common with a smooth, dense, and uniform film deposited on CdS. The optimum efficiency factor of the device can reach 6.06%, which is the highest value among $TiO_2/Sb_2S_3$ devices with a new short circuit current density record (19.4 mA $cm^{-2}$). The high electron transfer efficiency of $TiO_2$ treated with reactive ion etching is due to the high transparency of $TiO_2$ and $Sb_2S_3$ thin film of high quality with suppressed recombination in the $Sb_2S_3$ bulky film and the $TiO_2/Sb_2S_3$ interface. In addition, we propose a simple and effective strategy for depositing $Sb_2S_3$ thin films of high-quality on inert substrates [125].

The authors of [126] systematically studied the effect of close-spaced sublimation (CSS) temperature on the growth of the $Sb_2S_3$ absorber using a wide temperature range of 240–400°C. Temperatures above 320°C caused cracking (spalling) in the $Sb_2S_3$ absorbing film. 300°C was chosen as the optimum temperature for sublimation treatment at a short range, which made it possible to obtain uncracked $Sb_2S_3$ films with increased planar flatness (hk1) and to set up the best $CdS/Sb_2S_3$ device with a photoconversion efficiency of 3.8%. Temperature-dependent admittance spectroscopy (TAS) study showed up two deep defects with activation energies of 0.32 eV and 0.37 eV. The measurement of low-temperature photoluminescence revealed interband emission at 1.72 eV and a broad band with a maximum at 1.40 eV, which was referred to the recombination of a donor–acceptor pair.

As is known, the orientation of antimony sulfide ($Sb_2S_3$) significantly affects the characteristics of solar cells of $Sb_2S_3$-based thin-film due to the quasi-one-dimensional crystal structure specific to it [127]. Therefore, the production of $Sb_2S_3$ film with [hk1] orientation is theoretically favorable for the performance of the solar cells. However, preparing $Sb_2S_3$ film with the *[hk1] orientation* is a difficult task, because $Sb_2S_3$ tends to grow parallel to the substrate. In this work, the authors successfully control the orientation of the $Sb_2S_3$ film by modulating the grain growth process. $Sb_2S_3$ films with a high [hk1] orientation can be obtained on a CdS substrate if the grain grows according to the normal grain growth model. Therefore, the $Sb_2S_3$-based solar cell with the *[hk 1] orientation* achieves an energy-conversion efficiency of 6.82%, which is high than the $Sb_2S_3$-based solar cell with the *[hk0] orientation* (6.27%). This research provides a novel and efficient method for controlling the $Sb_2S_3$ orientation to obtain high-efficiency $Sb_2S_3$ thin-film solar cells.

The authors of [128] studied the effect of annealing on the structural and optical properties of antimony trisulfide ($Sb_2S_3$). $Sb_2S_3$ powder evaporates onto clean glass substrates at room temperature under high vacuum pressure forming thin films. Structural studies were carried out using X-ray diffraction (XRD) and atomic force microscopy (AFM). The transformation of these thin films from amorphous to polycrystalline was shown by X-ray diffraction analysis after thermal annealing. Also, the morphology of these films was explained. The absorption coefficient and the optical band gap of the studied films were calculated from the transmission spectra. According to the absorption spectra of the UV-visible range, both samples have strong absorption in the visible spectrum.

## Conclusion

The electrochemical deposition method for obtaining $Sb_2S_3$ thin films is currently widely used among the other methods. During the deposition process, ions existing in the electrolyte accept electrons from the cathode and are converted into neutral atoms or molecules that are deposited on the surface of the cathode. The deposited substance in a short time forms a film or coating on the cathode surface, which can have different properties depending on the electrolyte composition and deposition conditions. Using the electrochemical method, the thickness, composition, structure, and properties of $Sb_2S_3$ films can be precisely controlled in line with the parameters of the process, such as current, voltage, deposition time, electrolyte composition, and temperature. Also, electrodeposition can provide the synthesis of films with improved properties, such as to achieving high density, hardness, adhesion, corrosion resistance, and chemical stability.

An analysis of the literature and the experimental data presented in them show that although various elements were used for doping, most studies have focused on metal alloying (doping). The doping of the $Sb_2S_3$ thin films played a decisive role not only in the productivity gains of the solar cell device, but also in improving their operational life and other important characteristics. Thus, doping is a powerful strategy for tuning the band gap, the concentration of ionized donors, improving charge transfer and conductivity, as well as controlling crystallization in the $Sb_2S_3$ films. It is possible to fabricate translucent solar cells with high efficiency and excellent stability using doped $Sb_2S_3$ films.

## References

1. Aliev A.S., Mamedov M.N. Electrodeposition of thin layers of CdSe on a Pt electrode. *Известия высших учебных заведений. Химия и химическая технология- Izvestiya Vysshikh Uchebnykh Zavedenii Khimiya i Khimicheskaya Tekhnologiya*. 2007, no. 12, pp. 70-73.
2. Mamedov M.N., Aliev A.Sh. Electrical properties of electrodeposited CdTe thin films. *Inorganic Materials*, 2008, vol. 44, no. 8, pp. 804-806.

3. Aliev A.S., Mamedov M.N., Abbasov M.T. Photoelectrochemical properties of $TiO_2$/CdS heterostructures. *Inorganic Materials*, 2009, vol. 45, no. 9, pp. 965-967.
4. Zeynalova A.O., Javadova S.P., Majidzade V.A., Aliyev A.Sh. Electrochemical synthesis of iron monoselenide thin films. *Chemical Problems*, 2021, vol. 19, no. 4, pp. 262-271.
5. Smilyk V.O., Fomanyuk S.S., Rusetskiy I.A., Danilov M.O., Kolbasov G.Ya. Comparative analysis of electrochromic properties of $CuWO_4$•$WO_3$, $Bi_2WO_6$•$WO_3$ and $WO_3$ thin films. *Chemical Problems*, 2022, vol. 20, no. 4, pp. 289-296.
6. Eminov Sh.O., Tagiyev D.B., Aliyev A., Jalilova Kh.D., Guliyev J.A., Rajabli A.A., Mamedova G.H., Karimova A.Kh., Abdullayeva S.H., Majidzade V.A. Integration of supercapacitor with solar cell based on $NiO_2$ and CdS nanopillars embedded in porous anodic alumina templates. *International Journal of Energy Research*, 2022, vol. 46, issue 15, pp. 22134-22144.
7. Abdullayeva S.H., Eminov Sh.O., Jalilova Kh.D., Musayeva N.N., Guliyev J.A., Aliyev A.Sh., Majidzade V.A., Mammadova G.H. Synthesis of anodic $TiO_2$ nanotubes on Indium Tin Oxide coated glass electrodes. *International Journal of Energy Research*, 2022, vol. 46, issue 15, pp. 21686-21693.
8. Javadova S.P., Majidzade V.A., Aliyev A.Sh., Tagiyev D.B. Effect of major factors on the composition of thin $Bi_2Se_3$ films. *Russian journal of applied chemistry*, 2021, vol. 94, no. 1, pp. 38-42.
9. El-rouby M., Aliyev A.Sh. Electrical, electrochemical and photo-electrochemical studies on the electrodeposited n-type semiconductor hexagonal crystalline CdS thin film on nickel substrate. *Journal of Materials Science: Materials in Electronics*, 2014, vol. 25, no. 12, pp. 5618-5629.
10. Aliyev A.Sh., Elrouby M., Cafarova S.F. Electrochemical synthesis of molybdenum sulfide semiconductor. *Materials Science in Semiconductor Processing*, 2015, vol. 32, pp. 31-39.
11. Orudzhev F.F., Alikhanov N.M-R., Rabadanov M.Kh., Ramazanov Sh.M., Isaev A.B., Gadzhimagomedov S.Kh., Aliyev A.Sh., Abdullaev V.R. Synthesis and study of the properties of mag netically separable nanophotocatalysis $BiFeO_3$. *Chemical Problems*, 2018, vol. 16, no. 4, pp. 484-495.
12. Majidzade V.A., Mammadova S.P., Petkucheva E.S., Slavcheva E.P., Aliyev A.Sh., Tagiyev D.B. Co-electrodeposition of iron and sulfur in aqueous and non-aqueous electrolytes. *Bulgarian Chemical Communications*, 2020, vol. 52, Special no. E, pp. 73 – 78.
13. Jafarova S.F., Majidzade V.A., Kasimogli I., Eminov Sh.O., Azizova A.N., Tagiyev D.B. Electrical and Photoelectrochemical Properties of Thin $MoS_2$ Films Produced by Electrodeposition. *Inorganic Materials*, 2021, vol. 57, no. 4, pp. 331-336.
14. Javadova S.P., Majidzade V.A., Aliyev G.S., Aliyev A.SH., Tagiyev D.B. Mathematical modeling of the electrodeposition process of bismuth-selenium system.*Chemical Problems*, 2021, vol. 19, no. 1, pp. 47-55.
15. Majidzade V.A., Aliyev A.Sh. Electrodeposition of $Ni_3Bi_2Se_2$ Thin Semiconductor Films. *Iranian Journal of Chemistry and Chemical Engineering*, 2021, vol. 40, no. 4, serial number 108, pp. 1023-1029.
16. Majidzade V.A. Javadova S.P., Dadashova S.D., Aliyev A.Sh., Tagiyev D.B. Mathematical modeling and optimization of the process of formation of functional thin $MoSe_2$ films. *Mathematical Models and Computer Simulations*, 2023, vol. 5, no. 1, pp. 73-78.
17. Aliyev A.Sh., Tagiyev D.B., Majidzade V.A., Guseynova R.G. Synthesis, properties and applications of thin semiconductor films of cadmium chalcogenides**.** Baku:Elm Puble, 2020, 272 p.
18. Senthil T.S., Kalaiselvi C.R. New Materials for Thin Film Solar Cells. Chapter in Book “Coatings and Thin-Film Technologies” Edited by Jaime Andres Perez-Taborda and Alba G. Avila Bernal, 2019, 286 p. 10.5772/intechopen.74351
19. Chen Y., Yang Y., Chen X., Liu F., Xie T. Orientation-controllable growth of Sb nanowire arrays by pulsed

electrodeposition. *Mater. Chem. Phys*., 2011, vol. 126, no. (1-2), pp. 386-390.
20. Leimkuehler G., Kerkamm I., Reineke-Koch R. Electrodeposition of Antimony Telluride. *J. Electrochem. Soc.* 2002, vol. 149, no. 1, pp. C474-C478.
21. Xiao F., Hangarter C., Yoo B., Rheem Y., Lee K-H., Myung N.V. Recent progress in electrodeposition of thermoelectric thin films and nanostructures. *Electrochim. Acta*, 2008, vol. 53, pp. 8103-8117.
22. Majidzade V.A. The effect of various factors on the composition of electrolytic thin films Sb-Se *Chemical Problems*, 2018, vol. 16, no. 3, pp. 331-336.
23. Majidzade V.A., Guliyev P.H., Aliyev A.Sh. Elrouby M., Tagiyev D.B. Electrochemical characterization and electrode kinetics for antimony electrodeposition from its oxychloride solution in the presence of tartaric acid. *Journal of Molecular Structure*, 2017, vol. 1136, pp. 7-13.
24. Majidzade V.A., Aliyev A.Sh., Qasimogli İ., Quliyev P.H., Tagiyev D.B. Electrical properties of electrochemically grown thin $Sb_2Se_3$ semiconduc tor films**.** *Inorganic Materials*, 2019, vol. 55, no. 10, pp. 979–983.
25. Majidzade V.A., Aliyev A.Sh., Guliyev P.H., Babanly D.M. Electrodeposition of the $Sb_2Se_3$ thin films on various substrates from the tartaric electrolyte. *Electrochemical Science and Engineering*, 2020, vol. 10, no. 1, pp. 1-9.
26. Majidzade V.A. $Sb_2Se_3$-based solar cells: obtaining and properties. *Chemical Problems*, 2020, vol. 18, no. 2, pp. 181-198.
27. Majidzade V.A., Aliyev A.Sh., Tağıyev D.B. Electrochemical deposition of $Sb_2Se_3$ thin films semiconductor from tartaric acid solution. *Bulgarian Chemical Communications*, 2020, vol. 52, Special no. E, pp. 62 – 67.
28. Majidzade V.A., Aliyev G.S., Aliyev A.Sh., Huseynova R.H., Mammadova Z.M. Mathematical modeling and optimization of the electrodeposition process of antimony-selenium system. *Azerbaijan Chemical Journal*, 2021, no. 1, pp. 30-36.
29. Majidzade V.A., Javadova S.P., Aliyev G.S., Aliyev A.Sh., Tagiyev D.B. Electrodeposition of Sb–Se Thin Films from Organic Electrolyte. *Chemistry Africa*, 2022, vol. 5, no. 6, pp. 2085-2094.
30. Messina S., Nair M.T.S., Nair P.K. Solar cells with $Sb_2S_3$ absorber films. *Thin Solid Films*, 2009, vol. 517, no. 7, pp. 2503–2507.
31. Abd-El-Rahman K.F., Darwish A.A.A. Fabrication and electrical characterization of p-$Sb_2S_3$/n-Si heterojunctions for solar cells application. *Current Applied Physics*, 2011, vol. 11, no. 6, pp. 1265–1268.
32. Osuwa J.C., Osuji R.U. Analysis of electrical and micro-structural properties of annealed antimony sulphide ($Sb_2S_3$) thin films. *Chalcogenide Letters*, 2011, vol. 8, no. 9, pp. 571 - 577.
33. González-Lúa R., Escorcia-García J., Pérez-Martínez D., Nair M.T., Campos J., Nair P.K. Stable performance of chemically deposited antimony sulfide-lead sulfide thin film solar cells under concentrated sunlight. *ECS Journal Solid State Science and Technology*, 2015, vol. 4, no. 3, pp. 9-16.
34. Choi Y., Lee Y.H., Im S.H., Noh J.H., Mandal T.N., Yang W.S., Seok S.I. Efficient Inorganic-Organic Heterojunction Solar Cells Employing $Sb_2(S_x/Se_{1-x})_3$ Graded-Composition Sensitizers. *Advanced Energy Material*, 2014, vol. 4, no. 7, 1301680.
35. Ali N., Ahmed R., Haq B., Shaari A., Hussain R., Goumri-Said S. A novel approach for the synthesis of tin antimony sulphide thin films for photovoltaic application. *Solar Energy*, 2015, vol. 113, pp. 25-33.
36. Wan L., Ma C., Hu K., Zhou R., Mao X., Pan S., Wong L.H., Xu J. Two-stage co-evaporated $CuSbS_2$ thin films for solar cells. *Journal of Alloys Compound*, 2016, vol. 680, pp. 182-90.
37. Sun P., Yao F., Ban X., Huang N., Sun X. Directly hydrothermal growth of antimony sulfide on conductive substrate as efficient counter electrode for dye-sensitized solar cells. *Electrochemical Acta*, 2015, vol. 174, pp.127-32.
38. Choi Y.C., Yeom E.J., Ahn T.K., Seok S.I. $CuSbS_2$ Sensitized Inorganic–Organic Heterojunction Solar Cells Fabricated Using a Metal–Thiourea Complex Solution.

*Angew Chemical International Edition*, 2015, vol. 54, no.13, pp. 4005-4009.

39. Bansal N., Mahony F.T., Lutz T., Haque S.A. Solution Processed Polymer–Inorganic Semiconductor Solar Cells Employing $Sb_2S_3$ as a Light Harvesting and Electron Transporting. *Advanced Energy Materials*, 2013, vol. 3, no. 8, pp. 986-990.
40. Shah U.A., Chen Sh., Khalaf G.M.G., Jin Z., Song H. Wide Bandgap $Sb_2S_3$ Solar Cells // *Advanced Functional Materials*, 2021, vol. 31, no. 27, 2100265.
41. Bao H., Cui X., Li C.M., Song Q., Lu Z., Guo J. Synthesis and Electrical Transport Properties of Single-Crystal Antimony Sulfide Nanowires. *The Journal of Physical Chemistry C*, 2007, vol. 111, no. 45, pp.17131–17135.
42. Ţigaˇu N., Gheorghieş C., Rusu G.I., Condurache-Bota S. The influence of the post-deposition treatment on some physical properties of $Sb_2S_3$ thin films. *Journal of Non-Crystalline Solids*, 2005, vol. 351, no. 12-13, pp. 987–992.
43. Boughalmi R., Boukhachem A., Kahlaoui M., Maghraoui H., Amlouk M. Physical investigations on $Sb_2S_3$ sprayed thin film for optoelectronic applications. *Materials Science in Semiconductor Processing*, 2014, vol. 26, pp. 593–602.
44. Kriisa M., Krunks M., Oja Acik I., Kärber E., Mikli V. The effect of tartaric acid in the deposition of $Sb_2S_3$ films by chemical spray pyrolysis. *Materials Science in Semiconductor Processing*, 2015, vol. 40, pp. 867–872.
45. Moon S.-J., Itzhaik Y., Yum J.-H., Zakeeruddin S.M., Hodes G., Grätzel M. $Sb_2S_3$-Based Mesoscopic Solar Cell using an Organic Hole Conductor. *The Journal of Physical Chemistry Letters*, 2010, vol. 10, no .1, pp. 1524–1527.
46. Choi Y.C., Lee D.U., Noh J.H., Kim E.K., Seok S.I. Highly Improved $Sb_2S_3$ Sensitized-Inorganic-Organic Heterojunction Solar Cells and Quantification of Traps by Deep-Level Transient Spectroscopy. *Advanced Functional Materials*, 2014, vol. 24, no. 23, pp. 3587–3592.
47. Validžić I.L., Mitrić M., Abazović N.D., Jokić B.M., Milošević A.S., Popović Z.S., Vukajlović F.R. Structural analysis, electronic and optical properties of the synthesized $Sb_2S_3$ nanowires with small band gap/ *Semiconductor Science and Technology*, 2014, vol. 29, no. 3, 035007.
48. Myagmarsereejid P., Ingram M., Batmunkh M., Zhong Y.L. Doping Strategies in $Sb_2S_3$ Thin Films for Solar Cells. *Small*, 2021, vol.17, issue 39, 2100241, https://doi.org/10.1002/smll.202100241.
49. Farhana M.A., Manjceevan A., Bandara J. Recent advances and new research trends in $Sb_2S_3$ thin film based solar cells. *Journal of Science: Advanced Materials and Devices*, 2023, vol. 8, no. 1, 100533.
50. Manolache S.A., Duta A. The Development of Crystalline $Sb_2S_3$ Thin Films as A Component of the Three-Dimensional (3D) Solar Cells. *Romanian Journal of Information Science and Technology*, 2008, vol. 11, no. 2, pp.109-121.
51. Tigau N., Gheorghieş C., Rusu G.I., Condurache-Bota S. The influence of the post-deposition treatment on some physical properties of $Sb_2S_3$ thin films. *Journal of Non-Crystalline Solids*, 2005, vol. 351, pp.987–992.
52. Inbakumar S., Andavan P.M. Structural and optical analysis of plasma exposed and annealed $Sb_2S_3$ thin film. *Rasayan J. Chem*., 2017, vol. 10, no. 2, pp. 507 – 512.
53. Oommen R., Mathew J.N., Rajalakshmi U.P. Structural and morphological studies of $Sb_2S_3$ thin films. *Journal of Ovonic Research*, 2010, vol. 6, no. 6, pp. 259-266.
54. Mathew N.J., Oommen R., Rajalakshmi U.P., Sanjeevirajaa C. Investigations on the Se doped $Sb_2S_3$thin films. *Chalcogenide Letters*, 2011, vol. 8, no. 7, pp. 441 – 446.
55. Aousgi F., Kanzari M. Structural and optical properties of amorphous $Sb_2S_3$ thin films deposited by vacuum thermal evaporation method. *Current Applied Physics*, 2013, vol. 13, pp. 262-266.
56. Aousgi F., Dimassi W., Bessais B., Kanzari M. Effect of substrate temperature on the structural, morphological, and optical properties of $Sb_2S_3$ thin films. *Applied Surface Science*, 2015, vol. 350, pp. 19–24.
57. Aousgi F., Kanzari M. Study of the optical properties of the amorphous $Sb_2S_3$ thin films. *Journal of Optoelectronics and*

*Advanced Materials*, 2010, vol. 12, no. 2, pp. 227 – 232.

58. Sinaoui A., Trabelsi I., Chaffar Akkar F., Aousgi F., Kanzari M. Study of Structural, Morphological and Optical Properties of $Sb_2S_3$ Thin Films Deposited by Oblique Angle Deposition. *International Journal of Thin Films Science and Technology*, 2014, no. 1, pp. 19-25.
59. Aousgi F., Kanzari M. Effect of Chemical Etching of Substrates on the Properties of $Sb_2S_3$ Thin Film. *International Journal of Engineering Research & Technology* (IJERT) 2013, vol. 2 no. 12, pp. 2520-2525.
60. Boughalmi R., Boukhachem A., Kahlaoui M., Maghraoui H., Amlouk M. Physical investigations on $Sb_2S_3$ sprayed thin film for optoelectronic applications. *Materials Science in Semiconductor Processing*, 2014, vol. 26, pp. 593–602.
61. Ghraïri N., Aousgi F., Zribi M., Kanzari M. Comparative studies of the properties of thermal annealed $Sb_2S_3$ thin films. *Chalcogenide Letters*, 2010, vol. 7, no. 3, pp. 217-225.
62. Mahanty S., Merino J.M., Leon M. Preparation and optical studies on flash evaporated $Sb_2S_3$ thin films. *Technology A: Vacuum, Surfaces, and Films*, 1997, vol. 15, no. 6, pp. 3060–3064.
63. Medles M., Benramdane N., Bouzidi A., Sahraoui K., Miloua R., Desfeux R., Mathieu C. Raman and Optical Studies of spray pyrolysed $Sb_2S_3$ thin. *Journal of optoelectronics and advanced materials*, 2014, vol. 16, no. 5-6, pp. 726 – 731.
64. Medina-Montes M.I., Montiel-González Z., Mathews N.R., Mathew X., The influence of film deposition temperatur e on the subsequent postnnealing and crysta llization of sputtered $Sb_2S_3$ thin films. *Journal of Physics and Chemistry of Solids*, 2017, vol.111, pp.182-189.
65. Medina-Montes M.I., Montiel-Gonzalez Z., Paraguay-Delgado F., Mathews N.R., Mathew X., Structural, morphological and spectroscopic ellipsometry studies on sputter deposited $Sb_2S_3$ thin films. *J. Mater Sci: Mater Electron*, 2016, vol. 27, no. 9, pp. 9710-9719.
66. Ghraïri F., Aousgi N., Zribi M., Kanzari M. Studies of the properties of thermally annealed $Sb_2S_3$ thin films. *Optoelectronics and advanced materials – rapid communications*, 2009, vol. 3, no. 8, pp. 757 – 762.
67. Perales F., Lifante G., Agullo´-Rueda F., de las Heras C. Optical and structural properties in the amorphous to polycrystalline transition in $Sb_2S_3$ thin films. *J. Phys. D: Appl. Phys*. 2007, vol. 40, pp. 2440–2444.
68. Rajpure K.Y., Bhosale C.H. Effect of composition on the structural, optical and electrical properties of sprayed $Sb_2S_3$ thin films prepared from non-aqueous medium. *Journal of Physics and Chemistry of Solids*, 2000, vol. 61, pp. 561 – 568.
69. Rajpure K.Y., Bhosale C.H. Preparation and characterization of spray deposited photoactive $Sb_2S_3$ and $Sb_2Se_3$ thin films using aqueous and non-aqueous media. *Materials Chemistry and Physics*, 2002, vol. 73, no. 1-2, pp. 6–12.
70. Zhang L., Zhuang D., Zhao M., Gong Q., Guo L., Ouyang L., Sun R., Wei Y., Lyu X., Peng X. $Sb_2S_3$ thin films prepared by vulcanizing evaporated metallic precursors. *Materials Letters*, 2017, vol. 208, pp.58-61.
71. Yin Y., Wu C., Tang R., Jiang C., Jiang G., Liu W., Chen T., Zhu C. Composition engineering of $Sb_2S_3$ film enabling high performance solar cells. *Science Bulletin,* 2019, vol. 64, no. 2, pp. 136-141**.**
72. Tigau N. Influence of thermoannealing on crystallinity and optical properties of $Sb_2S_3$ thin films. *Cryst. Res. Technol*., 2007, vol. 42, no. 3, pp. 281–285, DOI 10.1002/crat.20061.
73. Tigau N. Substrate temperature effect on the optical properties of amorphous $Sb_2S_3$ thin films. *Cryst. Res. Technol*., 2006, vol. 41, no. 5, pp. 474–480.
74. Tang R., Wang X., Jiang C., Li S., Jiang G., Yang S., Zhu C., Chen T. Vacuum assisted solution processing for highly efficient $Sb_2S_3$ solar cells. *Journal of Materials Chemistry A*, 2018, vol. 34, pp. 1-6.
75. Bhosale C.H., Uplane M.D., Patil P.S., Lockhande C.D. Preparation and properties of sprayed antimony trisulphide films. *Thin Solid Films*, 1994, vol. 248, no. 2, pp. 137-139.

76. Tigãu N., Structural characterization and optical propertiesof annealed $Sb_2S_3$ thin films. *Rom. Journ. Phys., Bucharest*, 2008, vol. 53, no. 1–2, pp. 209–215.
77. Horoz S., Koc H., Sahin Ö. Investigation of Structural, Optical and Photovoltaic Properties of $Sb_2S_3$ Thin Films. *Cumhuriyet Sci. J.*, 2017, vol. 38, no. 3, pp. 588-593.
78. Ubale A.U., Ghugare T.B., Deshpande V.P., Ibrahim S.G., Mitkari A.V., Kadam S.K. Effect of annealing on the structural, electrical and optical properties of chemically deposited nanostructured $Sb_2S_3$ thin films. *Optoelectronics and Advanced Materials – Rapid Communications*, 2013, vol. 7, no. 3-4, pp. 219 – 224.
79. Habubi N., Chiad S.S., Hasan S.J. The Effect of Thickness on Some Optical Properties of $Sb_2S_3$ Thin Films Prepared by Chemical Bath Deposition. *Bagdad Science Journal*, 2010, vol. 7, no. 1, pp. 168-173.
80. Ubale A.U., Deshpande V.P., Shinde Y.P., Gulwade D.P. Electrical, Optical and structural properties of nanostructured $Sb_2S_3$ thin films deposited by CBD technique. *Chalcogenide Letters*, 2010, vol. 7, no. 1, pp. 101 – 109.
81. Chiad S.S., Ibrahim A.M.E., Habubi N.F. Annealing Effect on the Optical Properties of $Sb_2S_3$ Thin Films. *J. of university of Anbar for pure science*, 2011, vol. 5, no. 3, pp. 18-22.
82. Calixto-Rodriguez M., Martı´nez H., Pen Y., Flores O., Esparza-Ponce H.E., Sanchez-Juarez A., Campos-Alvarez J., Reyes P. A comparative study of the physical properties of $Sb_2S_3$ thin films treated with $N_2$ AC plasma and thermal annealing in $N_2$. *Applied Surface Science,* 2010, vol. 256, pp. 2428–2433.
83. Chalapathi U., Poornaprakash B., Ahn C.-H., Park S.-H. Rapid growth of $Sb_2S_3$ thin films by chemical bath deposition with ethylenediamine tetraacetic acid additive. *Applied Surface Science,* 2018, vol. 451, pp.1-18.
84. Chate P.A., Sathe D.J., Lakde S.D., Bhabad V.D. A novel method for the deposition of polycrystalline $Sb_2S_3$ thin films. *J. Mater Sci: Mater Electron*, 2016, vol. 27, no. 12, pp. 12599-12603.
85. Chate P.A., Lakde S.D. Characteristics of $Sb_2S_3$ Thin Films Deposited by a Chemical Method. *International Journal of Thin Films Science and Technology*, 2015, vol. 4, no. 3, pp. 237-242.
86. Deshpande M.P., Chauhan K., Patel K.N., Rajput P., Bhoi H.R., Chaki S.H. Study of $Sb_2S_3$ thin films deposited by SILAR method. *Materials Reseach Express*, 2018, vol. 5, 056410.
87. Parize R., Cossuet T., Appert E., Chaix-Pluchery O., Roussel H., Rapenne L., Consonni V. Synthesis and properties of $ZnO/TiO_2/Sb_2S_3$ core–shell nanowire heterostructures using the SILAR technique. *J. Cryst End Comm.*, 2018, vol. 20, pp. 4455-4462
88. Zhao B., Wan Z., Luo J., Han F., Malik H.A., Jia C., Liu X., Wang R. Efficient $Sb_2Se_3$ sensitized solar cells prepared through a facile SILAR process and improved performance by interface modification. *J. Applied Surface Science*, 2018, vol. 450, pp. 228–235.
89. Hector G., Eensalu J.S., Katerski A., Roussel H., Chaix-Pluchery O., Appert E., Donatini F., Acik I.O., Kärber E., Consonni V. Optimization of the $Sb_2S_3$ Shell Thickness in ZnO Nanowire-Based Extremely Thin Absorber Solar Cells. *Nanomaterials (Basel).*, 2022, vol. 12, no. 2, 198, 20 pages. doi: 10.3390/nano12020198. .
90. Gi E.K., Lee S.-J., Sung S.-J., Cho K.Y., Kim D.-H. Spin-Coating Process of an Inorganic $Sb_2S_3$ Thin Film for Photovoltaic Applications. *J. of Nanoscience and Nanotechnology*, 2016, vol. 16, pp. 10763–10766.
91. Asogwa P.U., Ezugwu S.C., Ezema F.I., Osuji R.U. Influence of Dip Time on The Optical and Solid State Properties of As-Grown $Sb_2S_3$ Thin Films. *Chalcogenide Letters*, 2009, vol. 6, no. 7, pp. 287 – 292.
92. Nwofe P.A., Chukwu J.N. Optimisation of Doped Antimony Sulphide ($Sb_2S_3$) Thin Films for Enhanced Device Applications. *Journal of nano- and electronic physics*, 2017, vol. 9**,** no. 5, 05007 (4pp).
93. Karade S.S., Banerjee K., Majumder S., Sankapal B.R. Novel application of non-

aqueous chemical bath deposited $Sb_2S_3$ thin films as supercapacitive electrode. *International journal of Hydrogen Energy,* 2016, vol. 41, no. 46, pp. 21278-21285.

94. Liu M., Gong Y., Li Z., Dou M., Wang F. A green and facile hydrothermal approach for the synthesis of high-quality semi-conducting $Sb_2S_3$ thin films. *Applied Surface Science,* 2016, vol. 387, pp. 790-795.

95. Vinayakumara V., Obregón Hernándeza C.R., Shajia S., Avellanedaa D.A., Aguilar Martineza J.A., Krishnana B. Effects of rapid thermal processing on chemically deposited antimony sulfide thin films. *Materials Science in Semiconductor Processing*, 2018, vol. 80, pp. 9–17.

96. Maghraoui-Meherzi H., Ben Nasr T., Kamoun N., Dachraoui M. Physical properties of chemically deposited $Sb_2S_3$ thin films. *Comptes Rendus Chimie*, 2011, vol. 14, pp. 471–475.

97. Mane R.S., Lokhande C.D. Chemical deposition method for metal chalcogenide thin films. *Materials Chemistry and Physics*, 2000, vol. 65, pp. 1–31.

98. Messina S., Nair M.T.S., Nair P.K. Solar cells with $Sb_2S_3$ absorber films. *Thin Solid Films*, 2009, vol. 517, pp. 2503–2507.

99. Murtaza G., Akhtar M., Malik M.A., O'Brien P. Aerosol assisted chemical vapor deposition of $Sb_2S_3$ thin films: Environmentally benign solar energy material. *Materials Science in Semiconductor Processing,* 2015, vol. 40, pp. 643–649.

100. Mane R.S., Sankapal B.R., Lokhande C.D. Non-aqueous chemical bath deposition of $Sb_2S_3$ thin // *Thin Solid Films*, 1999, vol. 353, pp. 29-32.

101. Ezema F.I., Ekwealor A.B.C., Asogwa P.U., Ugwuoke P.E., Chigbo C., Osuji R.U. Optical Properties and Structural Characterizations of $Sb_2S_3$ Thin Films Deposited by Chemical Bath Deposition Technique. *Turkish Journal of Physics*, 2007, vol. 31, pp. 205 – 210.

102. Ornelas-Acosta R.E., Shaji S., Avellaneda D., Castillo G.A., Das Roy T.K., Krishnan B. Thin films of copper antimony sulfide: A photovoltaic absorber material. *Materials Research Bulletin*, 2014, vol. 61, pp. 215–225.

103. Parize R., Cossuet T., Chaix-Pluchery O., Roussel H., Appert E., Consonni V. In situ analysis of the crystallization process of $Sb_2S_3$ thin films by Raman scattering and X-ray diffraction. *Materials & Design,* 2017, vol. 121, pp. 1-10

104. Rodríguez-Lazcano Y., Guerrero L., Gomez Daza O., Nair M.T.S., Nair P.K. Antimony chalcogenide thin films: chemical bath deposition and formation of new materials by post deposition thermal processing, Department of Solar Energy Materials, Centro de Investigación en Energía, UNAM, Temixco, Morelos 62580, MEXICO Superficies y Vacío 9, 1999, pp. 100-103.

105. Shaji S., Garcia L.V., Loredo S.L., Krishnan B., Aguilar Martinez J.A., Das Roy T.K., Avellaneda D.A. Antimony sulfide thin films prepared by laser assisted chemical bath deposition. *Applied Surface Science*, 2017, vol. 393, pp. 369–376.

106. Shaji S., Arato A., O'Brien J.J., Liu J., Alan Castillo G., Mendivil Palma M.I., Das Royand T.K., Krishnan B. Chemically deposited $Sb_2S_3$ thin films for optical recording. *J. Phys. D: Appl. Phys*. 2010, vol. 43, no. 7, 075404.

107. Horoz S., Sahin O., Synthesis, characterization and photovoltaic properties of Mn- doped $Sb_2S_3$ thin film. *Materials Science-Poland*, 2017, vol. 35, no. 4, pp. 861-867.

108. Arato A., Perez-Tijerina E., Das Roy T.K., Alan Castillo G., Krishnan B., Cardenas E. Carbon-doped $Sb_2S_3$ thin films: Structural, optical and electrical properties. *Solar Energy Materials & Solar Cells*, 2009, vol. 93, pp.33– 36.

109. Onyishi S.O., Nnabuchi M.N., Augustine C. Effect of concentration on the morphological and optical properties of dye-sensitized antimony sulphide ($Sb_2S_3$) thin film. *Global journal of engineering science and researches,* 2018 , vol. 10, no. 5, pp. 112-119.

110. Daly P.B., Barry F.J. Electrochemical nickel-phosphorous alloy formation. *Int.*

*Mater. Rev.* 2003, vol. 48, no. 5, pp. 326-338.

111. Avilez Garcia R.G., Meza Avendaño C.A., Pal M., Paraguay Delgado F., Mathews N.R., Antimony sulfide ($Sb_2S_3$) thin films by pulse electrodeposition: Effect of thermal treatment on structural, optical and electrical properties. *Materials Science in Semiconductor Processing*, 2016, vol. 44, pp. 91–100.
112. Yesugade N.S., Lokhande C.D., Bhosale C.H. Structural and optical properties of electrodeposited $Bi_2S_3$, $Sb_2S_3$ and $As_2S_3$ thin films. *Thin Solid Films*, 1995, vol. 263, no. 2, pp. 145-149.
113. Majidzade V.A., Javadova S.P., Jafarova S.F., Aliyev A.Sh., Tagiyev D.B. Electrochemical deposition of thin $Sb_2S_3$ films. *The Russian Journal Of Applied Chemistry*. 2022, vol. 95, no. 10, pp. 1627-1633. DOI 10.1134/S1070427222100147.
114. Subramanian S., Chithra lekha P., Pathinettam Padiyan D. Enhanced electrical response in $Sb_2S_3$ thin films by the inclusion of polyaniline during electrodeposition. *Physica B: Condensed Matter*, 2010, vol. 405, no. 3, pp. 925–931.
115. Wallace A.G., King R.P., Zhelev N., Jaafar A.H., Levason W., Huang R., Reid G., Bartlett P.N. Anodic $Sb_2S_3$ electrodeposition from a single source precursor for resistive random-access memory devices. *Electrochimica Acta*, 2022, vol. 432, 141162
116. Janosevic V., Mitric M., Savic J., Validzic I.L.J. Structural, Optical, and Electrical Properties of Applied Amorphized and Polycrystalline $Sb_2S_3$ Thin Films. *Metallurgical and Materials Transactions A*, 2015, vol. 47, no. 3, pp.1460-1468.
117. Diliegros-Godines C.J., Santos Cruz J., Mathews N.R., Pal M. Effect of Ag doping on structural, optical and electrical properties of antimony sulfide thin films. *J. Mater. Sci*. 2018, vol. 53, pp.11562–11573. https://doi.org/10.1007/s10853-018-2420-3
118. Dong Y., Li X., Liu Sh. Zhu Q., Zhang M., Li J.-G., Sun X. Optimizing formulations of silver organic decomposition ink for producing highly-conductive features on flexible substrates: The case study of amines. *Thin Solid Films*, 2016, vol. 616, pp. 635-642
119. Wu W., Shan B., Feng K., Nan H., Resistive switching behavior of $Sb_2S_3$ thin film prepared by chemical bath deposition. *Materials Science in Semiconductor Processing*, 2016, vol. 44, pp.18–22.
120. Lei H., Lin T., Wang X., Dai P., Guo Y., Gao Y., Hou D., Chen J., Tan Z. Copper doping of $Sb_2S_3$: fabrication, properties, and photovoltaic application. *J. Mater. Sci: Mater. Electron,* 2019, vol. 30, pp. 21106–21116. https://doi.org/10.1007/s10854-019-02481-9
121. Patrick C.E., Giustino F. Structural and electronic properties of semiconductor-sensitized solar-cell interfaces. *J. Adv. Funct. Mater*. 2011, vol. 21, pp. 4663–4667.
122. Rowe D.M., Handbook of Thermoelctrics, CRC publishers, Boca Raton, 199 p.
123. Caruso F., Fillip M.R., Giustiono F. Excitons in one dimensional van der Waals material: $Sb_2S_3$ nanoribbons. *Physical Review*, 2015, vol. 92, vol. 12, 125134.
124. Hong J.-Y., Lin L.-Y., Li X. Electrodeposition of $Sb_2S_3$ light absorbers on $TiO_2$ nanorod array as photocatalyst for water oxidation. *Thin Solid Films*, 2018, vol. 651, pp. 124-130
125. You F., Chen Sh., Ma T., Xiao F., Chen C., Hsu H.-Y., Song H., Tang J. Reactive Ion Etching Activating $TiO_2$ Substrate for Planar Heterojunction $Sb_2S_3$ Solar Cells with 6.06% Efficiency. *Energy Technology*, 2022, vol. 10, no. 12, 2200940. https://doi.org/10.1002/ente.202200940
126. Krautmann R., Spalatu N., Josepson R., Nedzinskas R., Kondrotas R., Gržibovskis R., Vembris A., Krunks M., Oja Acik I. Low processing temperatures explored in $Sb_2S_3$ solar cells by close-spaced sublimation and analysis of bulk and interface related defects. *Solar Energy Materials and Solar Cells*, 2023, vol. 251, 112139

https://doi.org/10.1016/j.solmat.2022.112139.
127. Wu Ch., Zhang L., Che B., Xiao P., Yang J., Wang H., Chu L., Yan W., Chen T. The role of grain growth in controlling the crystal orientation of $Sb_2S_3$ films for efficient solar cells. *J. Mater. Chem. A*, 2023, vol. 11, pp. 8184-8191
128. AL-Obeidi A.-H.H., AL-Maiyaly B.-K.H. Annealing effect on structural and optical properties of $Sb_2S_3$ thin film. *AIP Conference Proceedings*, 2023, vol. 2475, 090026; https://doi.org/10.1063/5.0123128

## ПОСЛЕДНИЕ ДОСТИЖЕНИЯ В ПОЛУЧЕНИИ И ИССЛЕДОВАНИИ ТОНКИХ ПЛЕНОК НА ОСНОВЕ $Sb_2S_3$

**В.А. Меджидзаде, С.Ф. Джафарова, С.П. Джавадова, А.Ш. Алиев, Д.Б. Тагиев**

*Институт Катализа и Неорганической Химии им. акад. М. Нагиева МНО Азербайджанской Республики*
*AZ 1143, пр. Г. Джавида 113, Baku, Azerbaijan*
*e-mail: vuska_80@mail.ru*

**Аннотация**: $Sb_2S_3$ стабилен в условиях окружающей среды и является перспективным полупроводниковым материалом для оптоэлектроники; исследуются его потенциальные возможности в солнечных элементах, фотодетекторах и других устройствах. Он имеет непрямую ширину запрещенной зоны примерно 1.7-1.9 эВ, в зависимости от кристаллической структуры, что делает его подходящим для поглощения видимого света и использования в солнечных батареях. $Sb_2S_3$ может существовать в различных кристаллических структурах, включая орторомбическую и гексагональную структуры. Кристаллическая структура может существенно влиять на электронные и оптические свойства, что позволяет адаптировать его свойства для конкретных приложений с помощью инженерии кристаллической структуры. Он также обладает хорошими оптическими свойствами, высокими коэффициентами поглощения в видимой и ближней инфракрасной областях спектра. Это делает его пригодным для применения в фотогальванике и фотодетекторах. Несмотря на то, что существуют различные методы получения этого материала, необходимы дальнейшие исследования и разработки для оптимизации его свойств, повышения производительности и изучения новых приложений.
**Ключевые слова:** полупроводники, $Sb_2S_3$, электроосаждение, тонкие пленки, свойства $Sb_2S_3$ пленок

## $Sb_2S_3$ ƏSASINDA NAZİK TƏBƏQƏLƏRİN ALINMASI VƏ TƏDQİQİNDƏ SON NAİLİYYƏTLƏR

**V.A. Məcidzadə, S.F. Cəfərova, S.P. Cavadova, A.Ş. Əliyev, D.B. Tağıyev**

*Azərbaycan Respublikası Elm və Təhsil Nazirliyi akad. M. Nağıyev adına Kataliz və Qeyri-üzvi Kimya İnstitutu*
*AZ 1143, H. Cavid pr. 113, Bakı, Azərbaycan*
*e-mail: vuska_80@mail.ru*

**Xülasə:** $Sb_2S_3$ təbiətdə stabil olub, optoelektronika üçün perspektivli yarımkeçirici materialdır. Onun günəş batareyalarında, fotodetektorlarda və digər cihazlarda potensial imkanları geniş araşdırılır. Kristal quruluşundan asılı olaraq təxminən 1.7-1.9 eV birbaşa olmayan qadağan olunmuş zolağın eninə malikdir ki, bu da onu görünən işığın udulması və günəş hücrələrində istifadə üçün əlverişli edir. $Sb_2S_3$ müxtəlif kristal quruluşlarda, o cümlədən ortorombik və heksaqonal quruluşlarda mövcud ola bilər. Onun kristal quruluşu elektron və optik xassələrinə əhəmiyyətli dərəcədə təsir göstərə bilər ki, bu da onun xassələrinin kristal quruluş mühəndisliyi vasitəsilə xüsusi tətbiqlər üçün uyğunlaşdırılmasına imkan verir. O, həmçinin yaxşı optik xassələrə, spektrin görünən və yaxın infraqırmızı sahələrində yüksək udma əmsallarına malikdir. Bu, onu fotoqalvanik və fotodetektor tətbiqləri üçün yararlı edir. Lakin bu materialın alınması üçün müxtəlif üsulların olmasına baxmayaraq, onun xassələrini optimallaşdırmaq, çıxımını artırmaq və yeni tətbiq sahələrini araşdırmaq üçün əlavə tədqiqatların aparılmasına ehtiyac duyulur.

**Açar sözlər:** yarımkeçiricilər, $Sb_2S_3$, elektrokimyəvi çökmə, nazik təbəqələr, $Sb_2S_3$ təbəqələrinin xassələri